UPGRADES TO THE FSSP-100 ELECTRONICS

Darren O'Connor
SPEC Incorporated, Boulder, Colorado

1. INTRODUCTION

The forward scattering spectrometer probe (FSSP) was developed in the 1970's (Knollenberg 1981). The FSSP model 100 has been the subject of intensive instrument performance analysis (e.g., Dye and Baumgardner 1984; Cooper 1988; Brenguier 1989; Field et al. 2003) and upgrades (Cerni 1983; Brenguier et al. 1998). Brenguier et al. (1998) added the ability to record the arrival time of each particle and decreased the deadtime (time the probe was inactive while the electronics processed a particle event) from 6 μs to essentially 0 μs. Baker (1992) used particle interarrival times to investigate droplet clumping in cumulus clouds. Field et al. (2003) found that there were two fairly distinct peaks in particle arrival times when the probe was operated in the presence of large ice particles. One peak they attributed to closely spaced particles that resulted from ice shattering on the probe inlet, and a second, larger peak that was generated by particles passing unimpeded through the sample volume.

In this paper we describe upgrades to the FSSP-100 that result in:

1. Reduced offset errors associated with the AC coupling and baseline restoration circuitry.
2. Recording of signal and qualifier peak amplitudes of every particle, along with the particle transit time through the laser beam and the arrival time of the particle.
3. Sub-sampling (approximately 2%) of particle events that are digitized and recorded at a 40 MHz sample rate. The resulting time series of both the Signal and Qualifier waveforms may be viewed in post processing, (viewed as if a high-speed digital oscilloscope were probing the Signal and Qualifier channels in real time).
4. Data recorded at the probe on a flash disk. Data can also be recorded on an external computer via Ethernet connection. A field programmable gate array (FPGA) and onboard 400 Mhz Linux processor are completely programmable using an Ethernet connection, making field modifications easy to implement.

2. BASELINE RESTORATION CIRCUIT UPGRADE

The traditional FSSP100 baseline restoration circuit is shown in **Figure 1** and the newly implemented baseline restoration circuit is shown in **Figure 2.**. In **Figure 1**, photodiode current into U1 is AC coupled through capacitor C4. This generates negative going pulses out U2 as particles pass through the FSSP 100 laser beam. C4 builds up a bias voltage as each particle event occurs, producing a baseline shift in the output of U2. During the pulse event, the previous baseline value is held at the output of U4, and is fed as an offset to U5. This removes the previously sampled baseline voltage from the final output of U5. When particles exit the beam, the DC bias due to C4 is fed to U3 as a positive voltage and forces its output to go high. Capacitor C3, is then charged until it matches he DC bias on C4. By feeding this voltage through the unity gain amplifier U4 and on to the input of U5, the baseline shift is subtracted off of U5's output.

Figure 3a is a simulation of the traditional baseline restoration circuit in the presence of several particle events. The large particle events are on the order of 500 μS, and are on the order of magnitude of the kind of signal durations that may occur

during shattering events. The blue signal is the ideal output voltage and the green signal is the baseline restored output voltage. The baseline restoration circuit is not able to completely remove the baseline shift during the large transit time events, and by the 3rd one, centered at roughly 1.1 mS, the offset between the ideal and baseline restored outputs is 10 mV. When the pulse ends, the 10 mV offset remains. In the interval from 1.35 ms to 1.75 ms, the offset is seen to decay back to nearly zero volts.

Figure 4a shows a small particle event occurring immediately after the last of the large particles that were seen in **Figure 3**. At 1.355 mS, a pulse of ideal amplitude 25 mV occurs, but the baseline restore circuit outputs 35 mV due to the component of baseline shift that the baseline restoration circuit has not removed. 540 μs later, another particle event of the same amplitude occurs, shown in **Figure 4b**. At this time, the baseline restoration circuit is seen to have fully removed the baseline shift.

Photodiode current (represented by current source Ipd) in the newly implemented baseline restoration circuit, shown in **Figure 2**, is amplified through U1, then through U2 and U3. The signal is DC coupled throughout this series of amplifiers. When no particles are present, transistor Q1 is turned on, and any DC bias out of U3 is fed into U4. U4 integrates the DC bias, producing a negative accumulated output voltage. This negative voltage is fed back to U3, thus subtracting the DC bias from the output of U3, where the signal is then measured with DC bias removed. When particle events occur, the SFSSP logic turns off transistor Q1, and capacitor C6 serves to hold the accumulated DC bias correction voltage.

The output of U3 is fed to an analog-to-digital converter (ADC) that requires a 0.1 V offset for proper operation. This offset is achieved by feeding a 0.1 V reference into the positive terminal of U4. In the simulations (discussed next), this 0.1 V is subtracted off for clarity.

The main errors in this circuit are due to two sources:

1. When switch Q1 is off, or open circuit, the bias current of U4 flows through C6. At a typical value of 6 μA, it produces approximately a volt per second across C6, which is amplified by a gain of two through U3. Thus, during a 500 μs particle event, approximately 1 mV of baseline shift occurs at the output of U3. For typical transit times in flight of 2-3 μS, the offset is only on the order of 5 μV.
2. The input offset voltage of U4 is amplified by a gain of two through U3. This is a maximum of 550 μV (100 μV typical), producing approximately 1 mV of offset out of U3 after the gain is applied.

Figure 3b shows the new baseline restoration circuit response to the same particle events analyzed for the traditional circuit. Due to U4's offset voltage, a fixed offset of 1.2 mV exists on the baseline restored (green) signal. At the end of the last large particle event, again centered at 1.1 ms, the offset voltage is –3.2 mV, a change of 2 mV from nominal.

Figure 4c shows a small particle event occurring immediately after the last of the large particles that were seen in **Figure 3**. At 1.355 mS, a pulse of ideal amplitude 25 mV occurs, but the new baseline restore circuit outputs 21.74 mV due to the component of baseline shift that the new baseline restoration circuit has not removed. This is roughly the same 3.2 mV offset seen at the peak of the previous particle. 540 μs later, another particle event of the same amplitude occurs, shown in **Figure 4b**. At this time, the baseline-restored output is at

23.04 mV, representing an 800 μV shift from the nominal fixed offset.

In summary, the new baseline restoration circuit allows the photodiode current to be DC coupled through the amplifier chain, using servo techniques to remove any DC biases from the signal. It further provides a 100 mV offset required by the SFSSP ADC. The new baseline restoration circuit kept simulated errors to within approximately 10%, while the traditional circuit produced errors as great as 40%. In some cases of very large crystal break up, undesired offsets have been observed. These offsets were removed in real--time by an automatic algorithm that looks for particle events that last too long. The reset capability is a further feature of the new electronics, allowing the transistor Q1 to be forced on for brief periods, thus integrating off any spurious DC offsets.

3. SIGNAL AND QUALIFIER EVENT TIME SERIES CAPTURES

The SFSSP uses high-speed memory in the FPGA to not only capture particle-by-particle data, but also to capture entire particle events. An example is shown in **Figure 5**, where at concentrations on the order of 10^5 per liter, three coincident particle events were captured. The two marked with horizontal red arrows would normally be measured as good particles, since the transit time would exceed the running average used to define the beam diameter (Dye and Baumgardner 1984), and the maximum Signal peak exceeds the Qualifier peak. The effect of these accepted particles is to incorrectly bias the average transit time towards too large a value, and to produce measured peak values that are biased towards large particles. The latter effect is due to the probe only measuring the largest peak during the coincident event. This is (currently) the case for the SFSSP when measuring particle-by-particle events, and is the case for the original FSSP as well.

The effects of coincidence on the FSSP have been analyzed in many studies, such as by Baumgardner et. al. (1985), Cooper (1988), Brenguier (1989), and Coelho et al. (2005). The SFSSP, which captures with full-particle events at known sub-sample rates (of total particle events) provides for an entirely new means of analyzing the FSSP 100. With these data the techniques proposed for handling coincidence may be verified and fine-tuned.

A further potential use of particle event captures (PEC) is to correct particle sizes of individual particles, taking into account the time response of the analog amplifiers and the measured transit time of individual particles. Correction methods have been suggested by others (Korolev et. al., 1985; Cooper, 1988; Coelho, et. al. 2005, part I). A method based on the PEC capability of the SFSSP is discussed next.

3.1 TRANSIT TIME CORRECTIONS

The SFSSP measures real time particle events, allowing for unique analysis of the effects of the analog circuitry low-pass filtering on the waveform. The filter performs exponential smearing with a time constant τ. The value used in simulations to match a measured waveform was τ = 0.64 uS. **Figure 6** shows two simulations plotted against a measured (green) PEC. The simulation on top assumes the laser beam intensity is exactly Gaussian, corresponding to a $1/e^2$ beam width of 420 um, plotted in blue. The black signal is the simulated response of the filter to this signal. The simulation on the bottom is a modified Gaussian, using the same $1/e^2$ beam width, but modified by a gain and offset of 1.3 and –0.37, respectively. Negative values were then set to 0. This was done to attempt to match the resultant filtered waveform more closely to the measured response, as the HeNe laser is likely not a pure Gaussian in its intensity pattern

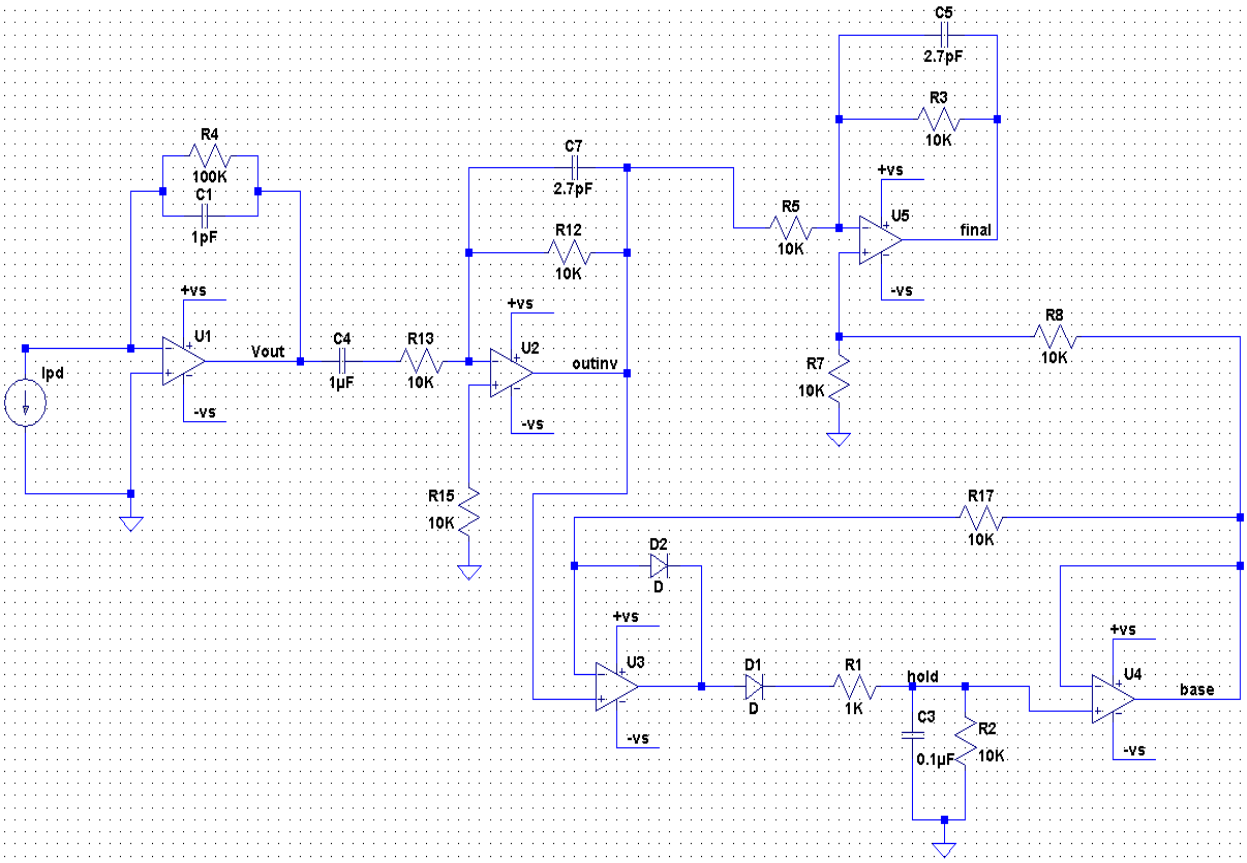

Figure 1. Traditional FSSP 100 front end amplifier (U1, U2) and baseline restoration (U3, U4, U5) circuitry. The Ipd current source models the photodiode behavior in the circuit.

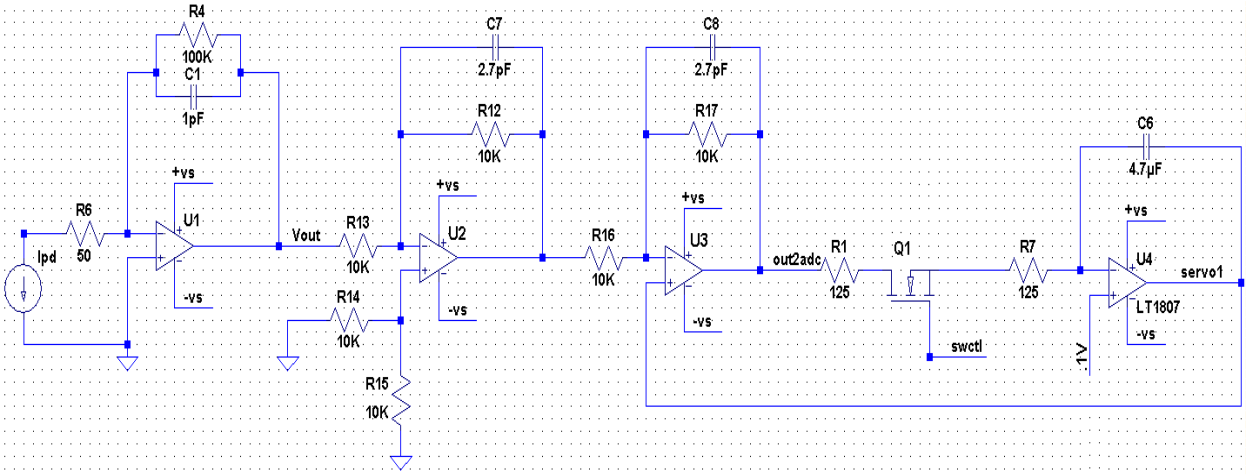

Figure 2. SPEC FSSP Upgrade front-end amplifiers (U1, U2 and U3) and new baseline restoration (U3, U4) circuitry. The Ipd current source models the photodiode behavior in the circuit.

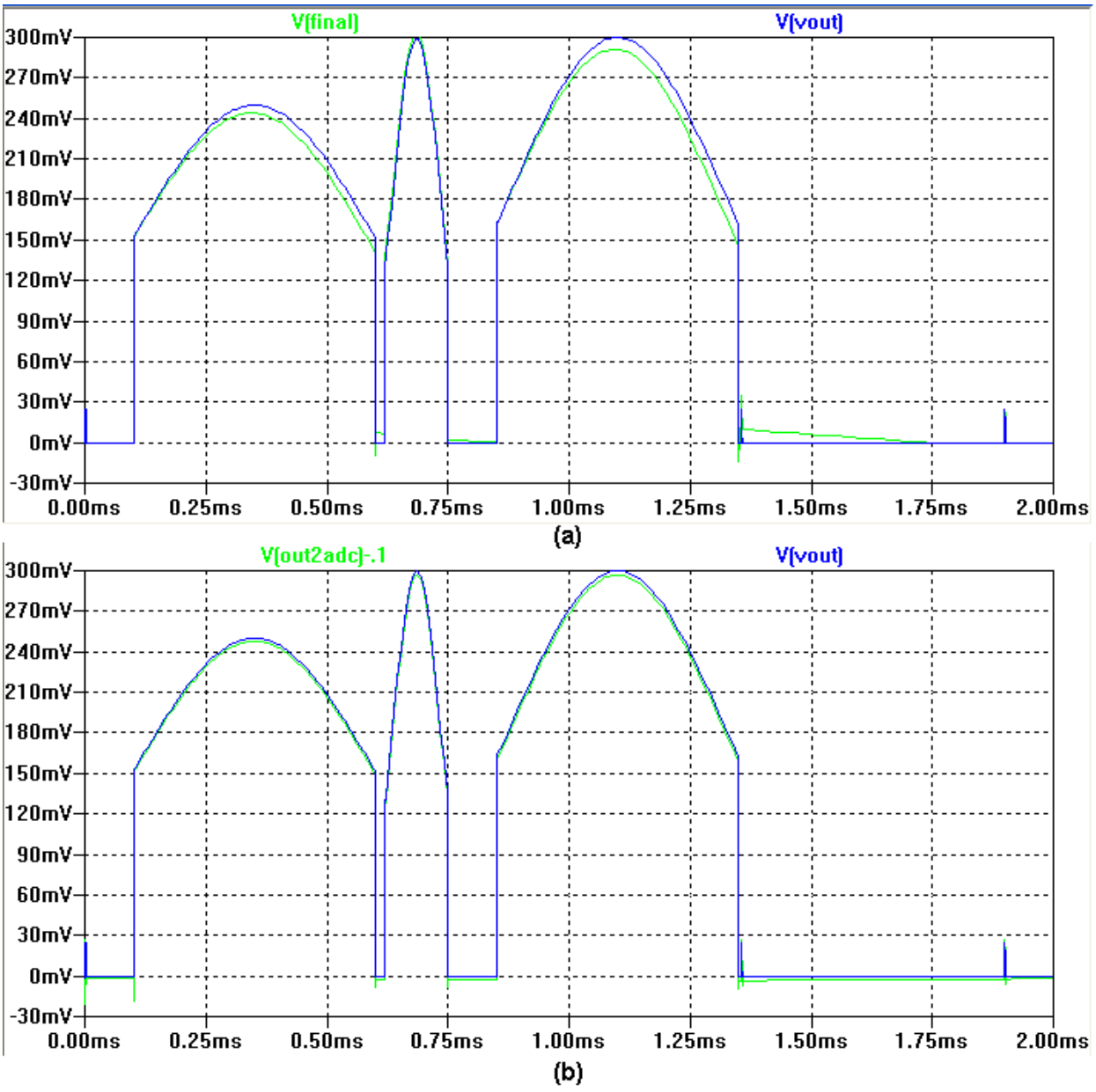

Figure 3. Ideal (blue) and baseline restored (green) signals for the traditional (a) and new (b) baseline restoration circuits. The large amplitude, long duration signals model shattering events.

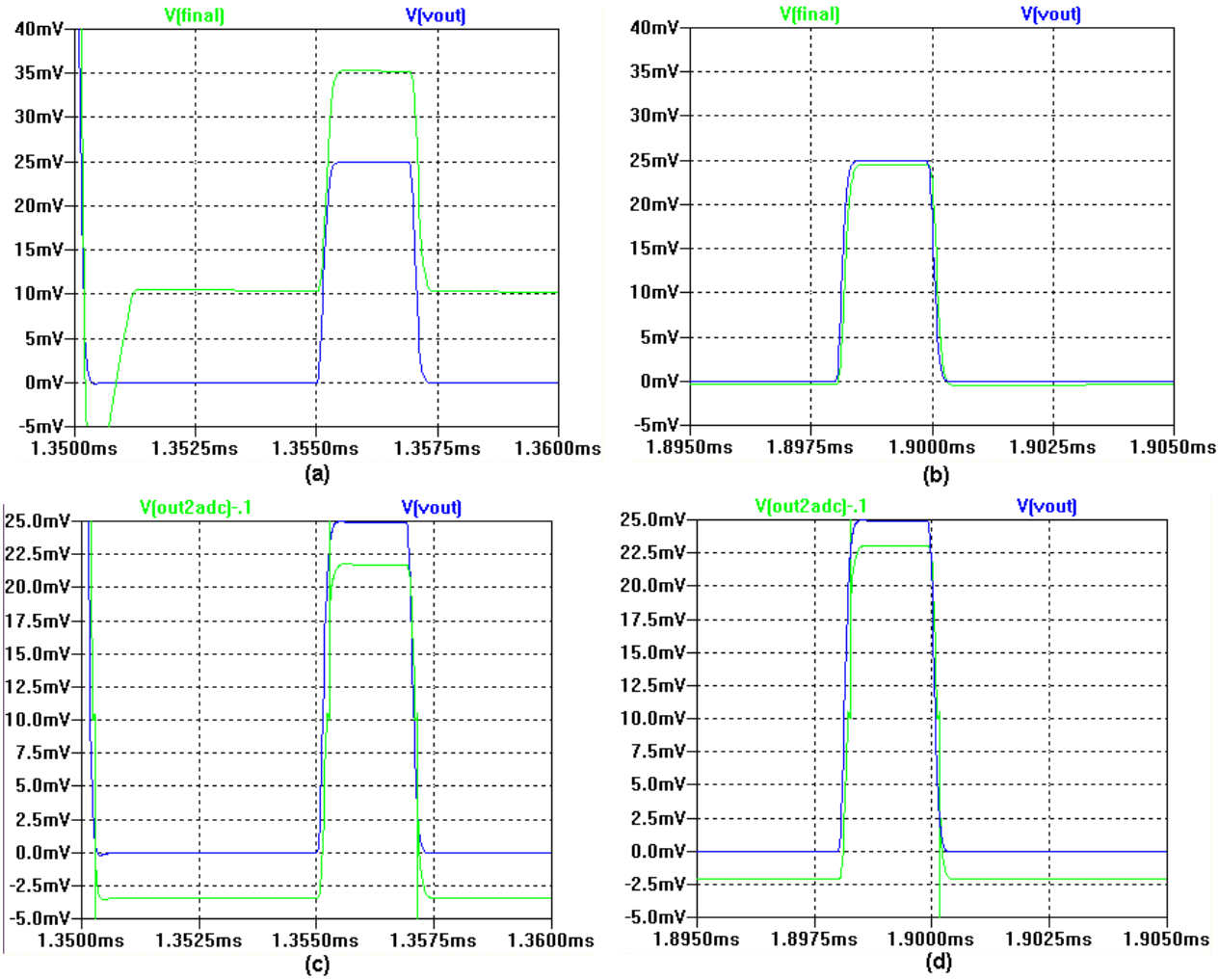

Figure 4. Ideal (blue) and baseline restored (green) signals for the traditional (a and b), and new (c and d) baseline restoration circuits. Plots (a) and (c) are for period immediately after the large signals in **Figure 3**. Plots (b) and (d) are 540 μs later.

Using a 20 mV threshold for the minimum at which a particle is detected, the transit times of the simulated signals is measured and estimated in several ways. The filtered signal period between the 20 mV limits is measured; the area under the curve, divided by the voltage peak for the same limits (20 mV) is estimated; and the time from the first (leftmost) 20 mV crossing to the peak is measured, and this value multiplied by two. The results for the two simulated waveforms are shown in **Table 1**.

Table 1. Estimates of transit time using measured time, area over peak, and time to peak (x2).

	Time, Real (us)	Time, Total (us)	% Error Total	Time, Area/Peak (us)	% Error Area/Peak	Time to peak x 2 (us)	% Error Time to Peak
Pure Gaussian	3.385	4.64	37	1.97	41.80	3.63	7.15
Modified Gaussian	2.45	4.67	96	1.85	24.5	3.11	27

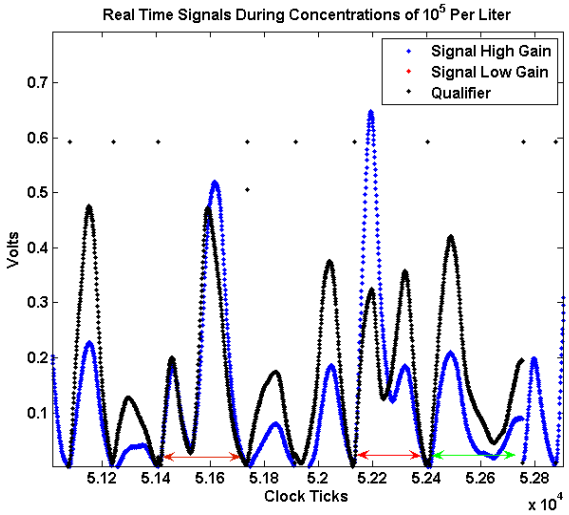

Figure 5. Total particle event captures by the SFSSP during concentrations of 10^5 per liter.

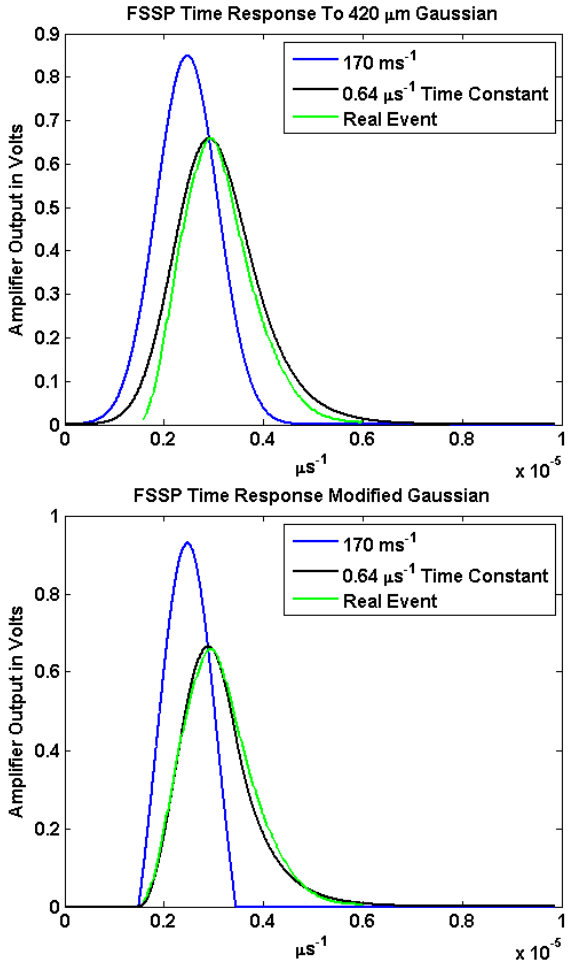

Figure 6. Simulated and measured FSSP waveforms. Blue is ideal (no exponential response smearing), black is with smearing (0.64 uS time constant), and green is a real measured event. Simulation done at 170 ms^{-1} to match assumed velocity of measurement. The top panel assumes the laser beam intensity is exactly Gaussian, corresponding to a $1/e^2$ beam width of 420 um. The bottom panel is a modified Gaussian, using the same $1/e^2$ beam width, but modified by a gain and offset of 1.3 and –0.37, respectively.

The area divided by the peak, assuming a uniform distribution for the laser, results in a transit time estimate of:

$$t' = t / (1 - e^{-t/\tau})$$

Where

t' = estimated transit time
t = true transit time
τ = time constant of the filter.

If τ is 3 times greater, or more, than the actual transit time, the estimated transit time will be smaller by 5% or less than the actual transit time.

As the laser intensity becomes less uniform and approaches a Gaussian, this result becomes less and less applicable. This is illustrated in **Table 1**, where the pure Gaussian result for the area / peak technique underestimates by 42%, while the modified Gaussian estimate is only off by 24.5%. Returning to **Figure 6**, one may notice that the modified Gaussian is closer in shape to a uniform distribution than is the pure Gaussian.

Since the two techniques bound the real transit time above (time to peak method) and below (area over peak method), the average of the two may yield better results. For the true Gaussian, the resultant error is 17.3%; for the modified Gaussian, the resultant error is 1.3%.

Figure 7 shows the percentage error for a modified Gaussian distribution while varying the velocity from 100 to 200 ms^{-1}. Using the average of the two techniques produces a worst case error of 9%. All three techniques greatly improve upon the total measurement that would otherwise be used.

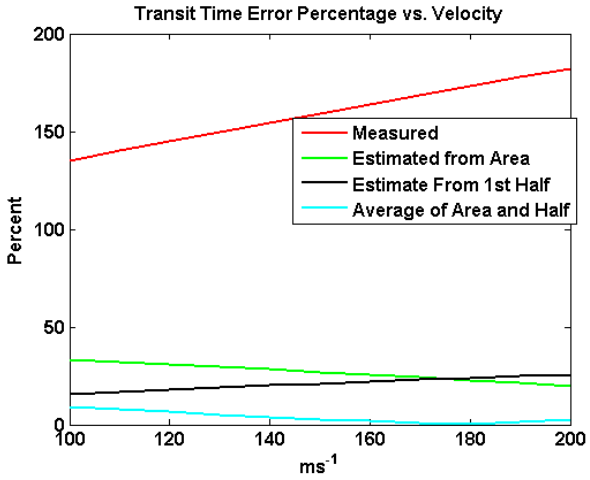

Figure 7. Absolute percentage error in estimating actual transit times across a 420 um $1/e^2$ Gaussian laser distribution. Errors are based on total measured transit time with no corrections (red); area under the voltage curve divided by the maximum voltage (green); transit time from the beginning to the peak times two (black); and average of the area / peak and peak times two methods (cyan).

3.2 PULSE HEIGHT CORRECTIONS

It is possible that with good transit time estimates, the decrease in the measured peak caused by the time response of the analog filter can be corrected. By simulating a range of particle sizes, as in **Figure 6**, the filtered peak (black in **Figure 6**) divided by the (assumed) real peak (blue in **Figure 6**) vs. transit time is seen to be a linearly decreasing value. This is seen in **Figure 8**, where the blue line is the ratio of measured to actual peak voltages vs. velocity of the simulated particle. The particle peak was 0.75 Volts. A least squares estimate of the blue curve, using the transit time estimated from the methods described above (average of area/peak and 1st half estimate) is also plotted in green.

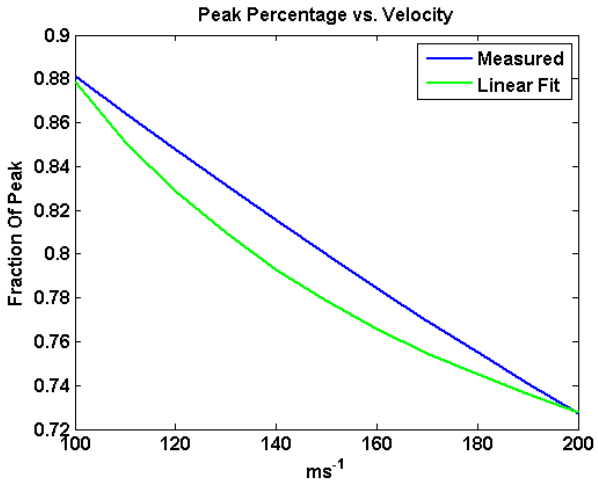

Figure 8. Ratio of measured peak to actual peak vs. velocity for 0.75 Volt signal.

Using the linear fit correction values from **Figure 8**, peak voltages are plotted in **Figure 9**. The actual peak voltage is plotted in blue, and the measured peak voltages vs. velocity are plotted in red. The corrected values vs. velocity are plotted in green. The maximum error in the estimate is less than 3%. Were one to perform a least squares fit for every simulation, this result would not be impressive or useful. However, the slope and offset values that generates the green line in **Figure8** works well for pulse heights ranging from 0.15 volts to 16 volts! At lower voltages, two other least squares fit values are used to cover the range of peaks from 20 mV to 150 mV, as the coefficients begin to change more rapidly in this pulse height region.

Measured signals from the FSSP allow analysis of this correction. For example, to correct the measured (green) signal on the right side of **Figure 6**, the transit time is first estimated to be 2.13 uS. This is different from the value in **Table 1**., because the simulated (black) signal was used to measure transit times in the table. Here, the real (green) signal is used and the pulse height of the simulated (blue) signal is then estimated from the following correction:

$$\text{Peak} = \text{measured peak} / (92292 \bullet \text{transit time}_{\text{estimate}} + 0.533)$$

Using the measured peak value of 0.659 volts and the estimated transit time of 2.13 us, the pulse height is estimated to be 0.90 volts. If one assumes the blue signal matches the original signal, before filtering, then the actual peak is close to its value: 0.85 volts. Without correction, the sizing error is –22.5%. After transit time correction, the error is 6.2%.

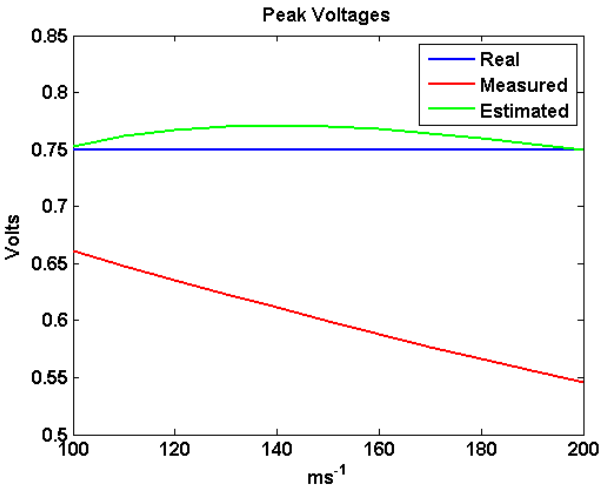

Figure 9. Real (blue), measured (red) and corrected estimate (green) peak values for a particle moving through the simulated FSSP at 100 to 200 meters per second.

To further test the peak estimate two more particle events are shown in **Figures 10** and **11**. The measured PEC (green) signals in the two figures have peak values of 0.27 and 6.22, spanning a broad range of voltages due to large differences in particle sizes. The simulated peak values, without filtering, are 0.4 volts and 8.1 volts for the blue plots in **Figures 10** and **11**. The estimate of the peak for the signals in **Figure 10**, using the transit time correction in EQ(1), is 0.4 volts. This is an error of only 0.2%, compared to the original 33% underestimate . The estimate of the peak for the signal in **Figure 11** is 8.49 volts, a 4.9% overestimate, compared to the original 6.22 volt, 23% underestimate.

Although the corrected peak values are being compared to simulated waveforms (modified Gaussians), the results are still likely to represent an improvement in accuracy. Assuming the modified Gaussians are the correct signal, the errors for three different simulations were reduced from 22.5% to 6.2% (**Figure 6**), from 33% to 0.2% (**Figure 10**), and from 23% to 4.9% (**Figure 11**).

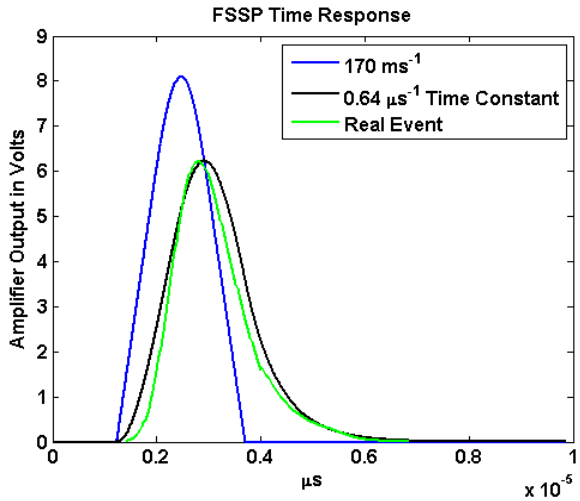

Figure 10. Measured signal (green) and simulated modified Gaussian without (blue) and with (black) filter effects. Actual Peak: 0.4, Measured Peak: 0.27 (33% low), Estimated Peak: 0.4 (0.2% over**)**

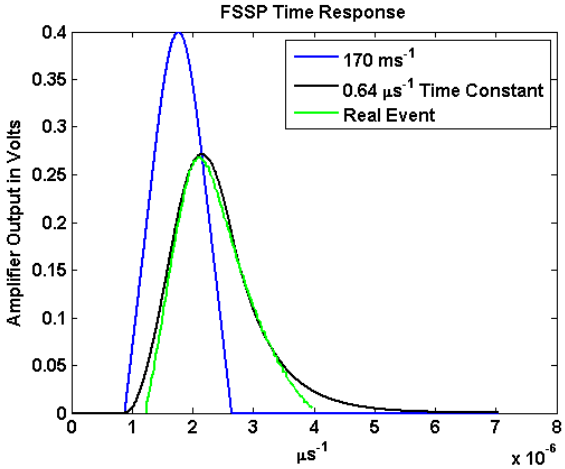

Figure 11. Measured signal (green) and simulated modified Gaussian without (blue) and with (black) filter effects. Actual Peak: 8.1, Measured Peak: 6.22 (23% low), Estimated Peak: 8.50 (4.9% high).

The SFSSP measures transit times three ways for particle by particle events:

1. Total transit time: the time it takes for a particle to rise above a minimum threshold of 10 mV, and to then fall below 5 mV. This method greatly overestimates transit times at aircraft speeds due to analog filter smearing of the signal during signal decay.
2. Time to peak: the time it takes for a particle to rise from the 10mV threshold to the peak. This method overestimates transit times, but by much less than the total transit time method.
3. Area / Peak Voltage: the area under the curve for the entire particle event is recorded. Dividing this value by the peak voltage yields an underestimate of the total transit time.

By using methods 2 and 3, and by determining the coefficients in EQ(1) from the PEC data, a particle by particle correction to size may be implemented.

A more exhaustive method may be implemented using the techniques by which figures 6, 10 and 11 were generated. It involves estimating the original particle size by generating a modified Gaussian time series, simulating the low-pass filtering effect of the analog electronics on this series, and comparing the filtered output to the original PEC event. The peak of the modified Gaussian, before filtering, is the resultant estimate of the particle peak without the attenuating effect of the filter.

3.3 AN EXAMPLE OF ICE CRYSTAL SHATTERING

Here we examine an example of ice crystal shattering from the recent DOE Atmospheric Radiation Measurement (ARM) ISDAC field project staged from Fairbanks, Alaska in April 2008. ISDAC Research Flight #32 included data collection by the Canadian NRC CV-580 research aircraft in cirrus clouds. **Figure 12**. shows the "wait time" (hereafter called w8 time) distribution from ISDAC flight #32. The ordinate is plotted as dN/dln(w8), where N is the number of particle events and a "tick" corresponds to one 25 ns clock period. The peak ending at approximately 30,000 w8 ticks indicates potential shattering events were prevalent at w8 times of this length and shorter (Field et. al. 2003). At the recorded aircraft speed of 138 ms^{-1}, this corresponds to an inter-arrival distance of 103.5 mm between particles. **Figures 13** and **14** are images captured by the SPEC CPI during this time period; **Figure 15** shows images captured by the SPEC 2D-S probe.

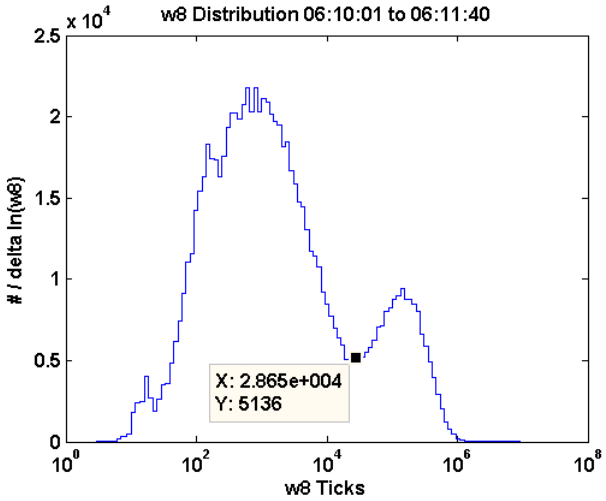

Figure 12. Inter-Arrival (w8) time / ln (w8 bin widths) distribution plotted vs. w8 ticks.

Figure 16 shows the particle size distribution for this period with all DOF and velocity average accepted particles (red), and without particles that have an inter-arrival time less than 30,000 clock periods (green). **Figure 17** shows the percentage of particles removed from the concentration distribution for each bin. The percent removed is relatively equal for all the bins, except for bins 2 and 3, corresponding to particle sizes between 1 and 5 μm. A possible explanation is that a real peak in the size distribution exists in these small sizes, and that most of the rest that were removed were due to shattering of larger particles. Both time periods in **Figure 17** show a clustering of particle events, which is to be expected in a period of shattering.

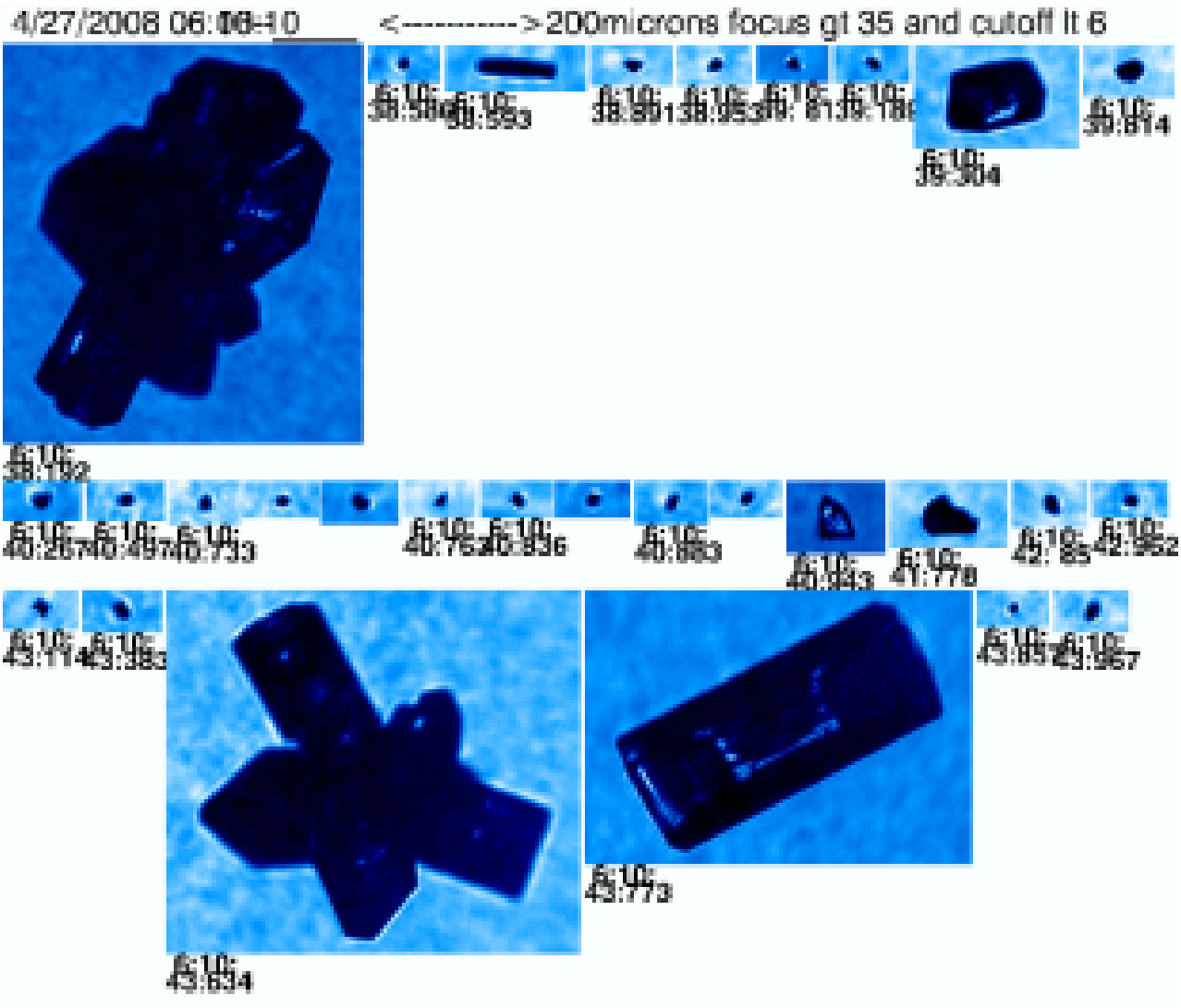

Figure 13. CPI images captured at approximately 06:10:44 during flight 32.

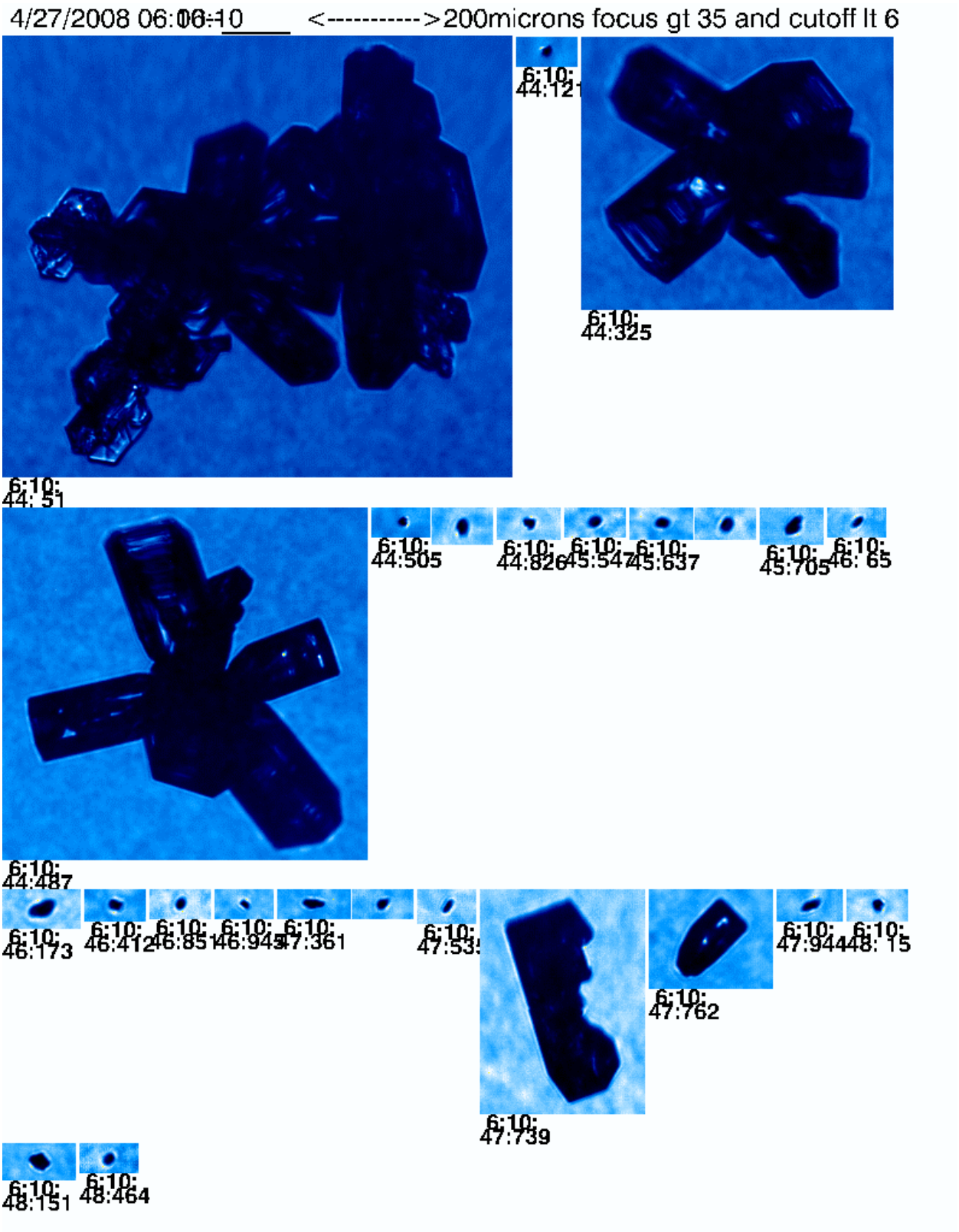

Figure 14. CPI images captured at approximately 06:10:48 during flight 32.

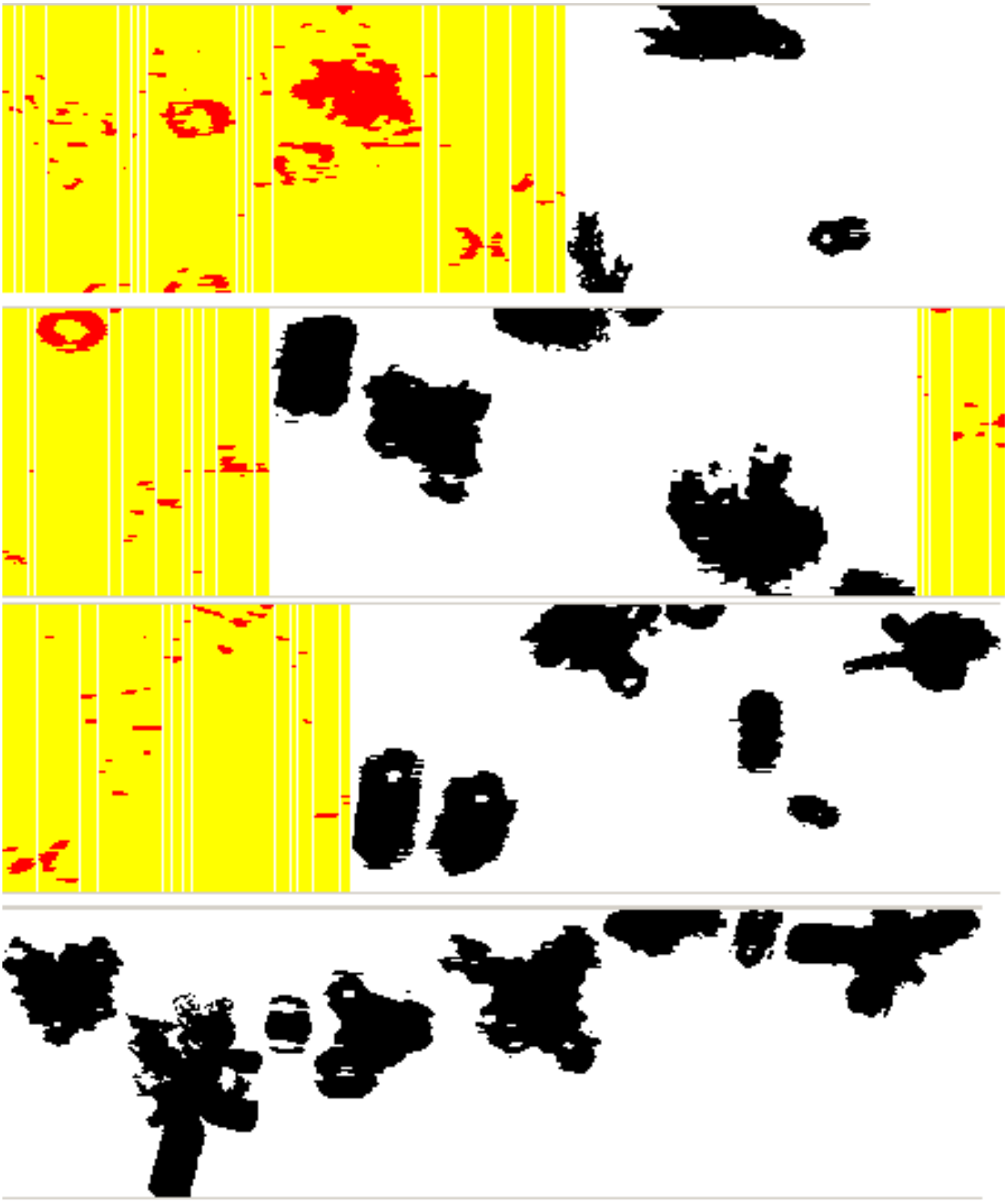

Figure 15. 2D-S images during period of interest. Heights of image strips are 1.28 mm. 2D-S shattering removal algorithms remove particles highlighted yellow.

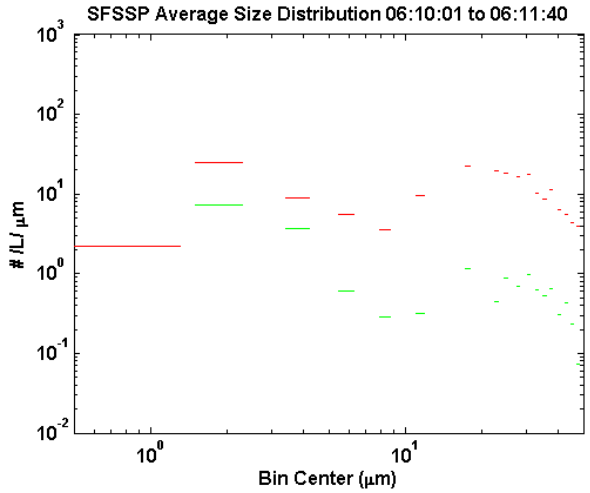

Figure 16. Average size distribution with velocity averaging accept and DOF accept limits (red), and with w8 time minimum of 30,000 ticks (green), or 103.5 mm.

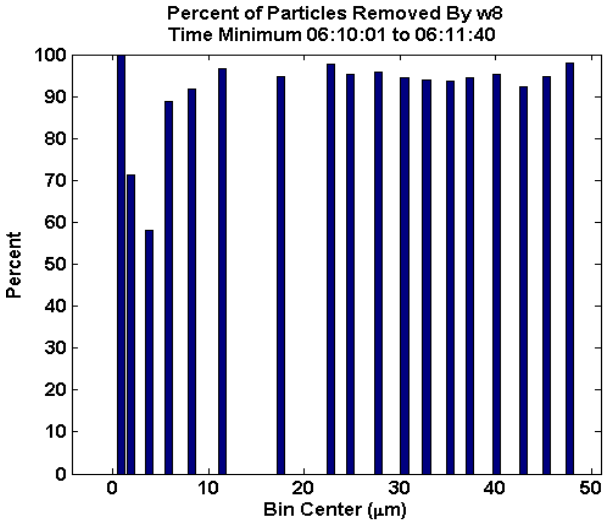

Figure 17. Percentage of concentration removed from each size bin by using the wait time minimum of 30,000 ticks = 103.5 mm.

Figures 18 and **19** show periods of particle event captures within the 100 second interval from which the average distributions in **Figure 16** were made. In **Figure18**, only one DOF accepted particle event is observed, with the signal channel voltage greater than the qualifier channel voltage. This one good particle would be sized in the 1 to 2.8 micron bin, where the peak in the distribution occurs in **Figure 1**. **Figure19** shows a very long PEC corresponding to a signal that goes high and stays high for much longer than the transit time of a single particle. The PEC in fact fails to record the entire event due to a limit on the amount of high speed memory devoted to capturing them. Clearly such a signal will bias the average transit time above the value that single particle transits would generate.

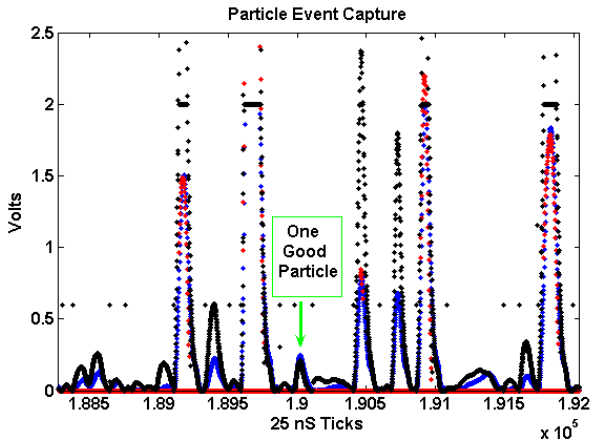

Figure 18. Real time signals (Signal channel in blue and red, Qualifier in black) within 06:10:01 to 06:11:40 period on flight 30.

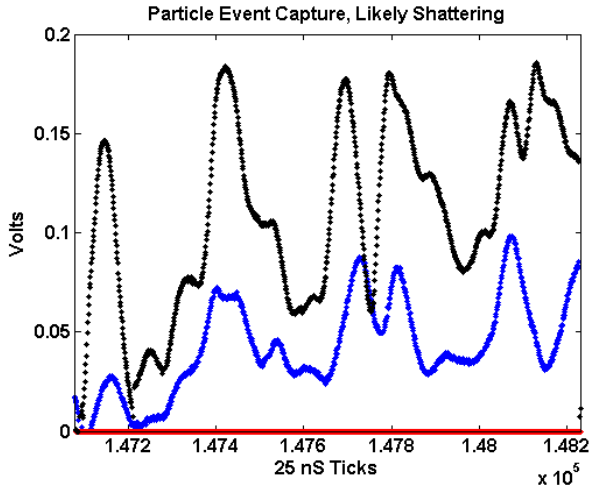

Figure 19. Real time signals (Signal channel in blue (high gain) and red(low gain), Qualifier in black) within 06:10:01 to 06:11:40 period on flight 32. Most of the time series is a single particle event.

4. SUMMARY

New electronics upgrades to the FSSP-100 are discussed. The new upgrades (i.e., the SFSSP probe) contain advanced technology enabling several improvements that make it possible to better understand instrument response.

Initial tests of an improved baseline restoration circuit show the new method works well. High concentrations are not expected to greatly alter the measured size distribution. Real time electronics monitors and resets the baseline when erroneous data occurs. The new baseline restoration circuit keeps simulated errors to within approximately 10%, while the traditional circuit produced errors as great as 40%.

The SFSSP has the unique ability to digitize and store both the signal and qualifier waveforms. By analyzing the time series from these waveforms, it is possible to correct transit time and pulse height measurements. The transit time is corrected for effects of the analog circuitry low-pass filtering on the waveform. Once the transit time is corrected, the decrease in measured peak voltage caused by the time response of the analog filter is corrected.

The SFSSP measures the arrival time of each individual particle. Using a technique similar to that described by Field et al. (2003), ice crystals that are suspected to have shattered on the probe inlet are removed by examination of their interarrival times. An example of shattered particle removal from the recent ISDAC field project is presented and discussed.

REFERENCES

Baker, B.A., 1992: Turbulent entrainment and mixing in clouds: A new observational approach, *J. Atmos. Sci.,* **49,** 387-404.

Baumgardner, D., Strapp, W., and Dye, J. E. 1985: Evaluation of the Forward Scattering Spectrometer Probe. Part II: Corrections for Coincidence and Dead—Time Losses. *J. Atmos. Oceanic Technol*., **2**, 626—632.

Brenguier, J. L., 1989: Coincidence and dead-time corrections for particle counter. Part II: High concentration measurements with an FSSP. *J. Atmos. Oceanic Technol.*, **6,** 585—598.

Brenguier, J-L., T. Bourrianne, A. de Araujo Coelho, J. Isbert, R. Peytavi, D. Trevarin, and P. Wechsler, 1998: Improvements of droplet size distribution measurements with the fast-FSSP. *J. Atmos. and Oceanic Tech*., **15**, 5, 1077-1090.

Cerni, T. A. 1983: Determination of the size and concentration of cloud drops with an FSSP. *J. Clim. & Appl. Meteorol*., **22**, 1346-1355.

Coelho, A., J-L. Brenguier, and Thierry Perrin: 2005: Droplet Spectra Measurements with the FSSP-100. Part I: Low Droplet Concentration Measurements. *J. Atmos. Oceanic Technol*. **22**, 1748—1755.

Coelho, A., J-L. Brenguier, and Thierry Perrin: 2005: Droplet Spectra Measurements with the FSSP-100. Part II: Coincidence Effects. *J. Atmos. Oceanic Technol*. **22**, 1756—1761.

Cooper, W. A., 1988: Effects of coincidence on measurements with a Forward Scattering Spectrometer Probe. *J. Atmos. Oceanic Technol*., **5**, 823—832.

Field, P., Wood, R., Brown, P. R. A., Kaye, P. H., Hirst, E., Greenway, R, and Smith, J. A., 2003: Ice Particle Interarrival Times Measured with a Fast FSSP. . *J. Atmos. Oceanic Technol*. **20**, 249—261.

Korolev, A. V., Makarov, Y. E., and Novikov, V. S., 1985: On the accuracy of photoelectric cloud droplet spectrometer FSSP—100., *Trans. Of Central Aerological Observatory (Trudi TsA0)*, 32—42.